FLUCOME 2009
10th International Conference on Fluid Control, Measurements, and Visualization
August 17–21, 2009, Moscow, Russia

DEVELOPMENT OF WALL SHEAR STRESS IN GÖRTLER VORTEX FLOW

S. H. Winoto[1], Tandiono[2], and D. A. Shah[2]

ABSTRACT

The development of wall shear stress in Görtler vortex flow was investigated by hot-wire measurements. The wavelengths of the vortices were pre-set by thin vertical perturbation wires so to produce the most amplified wavelengths. Three different vortex wavelengths of 12 mm, 15 mm, and 20 mm were considered, and near-wall velocity measurements were carried out to obtain the "linear" layers of velocity profiles in the boundary layers. The wall shear stress coefficient C_f was estimated from the velocity gradient of the "linear" layer. The spanwise-averaged wall shear stress coefficient $\overline{C}_f$, which initially follows the Blasius curve, increases well above the local turbulent boundary layer value further downstream due to the nonlinear effect of Görtler instability and the secondary instability modes. Three different regions are identified based on the streamwise development of $\overline{C}_f$, namely linear, nonlinear, and transition to turbulence regions. The onset of nonlinear region is defined as the streamwise location where the $\overline{C}_f$ begins to depart from the Blasius curve. In the nonlinear region, the spanwise distribution of C_f at the downwash becomes narrower, and there is no inflection point found further downstream.

Keywords: Görtler vortex flow, wall shear stress

INTRODUCTION

Görtler vortex flow is boundary layer flow on concave surface in the presence of streamwise counter-rotating Görtler vortices (Görtler, 1940). In such flow, high momentum fluid moves toward the surface giving rise to thinner boundary layer and higher shear stress at the so-called downwash, while at the so-called upwash, low momentum fluid moves away from the wall giving rise to thicker boundary layer and lower shear stress. Such boundary layer flow is relevant in applications, such as turbine blades, airfoils, and heat transfer enhancements, in which the wall shear stress τ_w becomes important. The presence of Görtler vortices will cause the friction drag to increase in the nonlinear region, especially when the secondary instability appears in the boundary layer.

The methods to measure τ_w have been discussed for example by Winter *et al*. (1979) and Hanratty and Campbell (1983). However, a brief description on the use of hot-wire to measure streamwise velocity near a wall in order to estimate the wall shear stress is provided here.

Hot-wire velocity measurements in the viscous sublayer to estimate the wall shear stress in turbulent boundary layer are generally associated with large methodological problems in the inner portions of the viscous sublayer. The setback is that the velocity in the sublayer is relatively small, and

[1] Corresponding author: Department of Mechanical Engineering, National University of Singapore, e-mail: mpewinot@nus.edu.sg

[2] Department of Mechanical Engineering, National University of Singapore

the heat loss due to free convection from the hot-wire may give rise to erroneous readings. However, the hot-wire measurements in the viscous sublayer have been reported, for example by Bhatia *et al*. (1982), Alfredsson *et al*. (1988), and Chew *et al*. (1994) who also obtained mean wall shear stress using hot-wire probe with its active element placed just above the wall within viscous sublayer.

Another problem is the very thin viscous sublayer so the probe may block the flow. The length (l) of the active hot-wire element has to be sufficiently large to achieve a length-to-diameter (l/d) ratio greater than 200 (Ligrani and Bradshaw, 1987a). On the other hand, l has to be sufficiently small to avoid the spatial resolution problems. Ligrani and Bradshaw (1987b) showed that the turbulence intensity, flatness factor, and skewness factor of the streamwise velocity fluctuations are independent of wire length as long as the non-dimensional wire length $l^+ (\equiv l u_\tau / \nu)$ does not exceed 20-25.

Unlike flat plate boundary layers, there is dearth of τ_w results in concave surface boundary layer which can be due to the difficulties associated with direct measurement. The reported results were mainly obtained from curve-fitting of the velocity data across boundary layer at the upwash and downwash wherein only few points near the wall were considered so that the τ_w may not be accurately estimated. In the nonlinear region, τ_w is found to rise and finally exceed the corresponding value for the turbulent boundary layer on a flat plate (Swearingen and Blackwelder, 1987; Ajakh *et al*., 1996).

The increase of τ_w in the nonlinear region of Görtler instability has also attracted much attention (Sabry and Liu, 1991; Hall and Horseman, 1991; Girgis and Liu, 2006). The computational results of Sabry and Liu (1991), who studied the nonlinear effects of Görtler vortices via a prototype problem, showed good qualitative agreement with the measurement of Swearingen and Blackwelder (1987). Hall and Horseman (1991) approximated the results of Swearingen and Blackwelder (1987) up to a certain streamwise distance through the study of the linear inviscid secondary instability of Görtler vortices. Recently, Girgis and Liu (2006) focused on the nonlinear modification of the steady flow by Reynolds stresses of wavy disturbance, and found that the τ_w increased well beyond the local turbulent values as the flow developed downstream due to the presence of the secondary instability modes.

The aim of this work is to provide more extensive experimental wall shear stress data in Görtler vortex flow. The data will be obtained from near-wall hot-wire measurements using the near-wall velocity gradient technique (Hutchins and Choi, 2002).

DESCRIPTION OF EXPERIMENT

The experiments were conducted in a 90° curved plexiglass test section connected to a low speed, blow down type wind tunnel (Fig. 1), with a rectangular cross-section of 150 mm x 600 mm. For flow control, a honeycomb and 5 rectangular fine-mesh screens with decreasing mesh-sizes from 500 to 180 μm are placed in the settling chamber prior to the contraction. The contraction consists of a 300 mm straight channel of 600 mm × 600 mm cross-section and a two-dimensional contraction of 4:1 ratio which reduces the cross-section to 150 mm x 600 mm. A concave surface of radius of curvature R = 1.0 m is mounted in the curved test section by means of slots at the side walls at a distance of 50 mm from its bottom surface. The distance between the concave surface and its top cover is 100 mm. The wind tunnel and the test section are connected by a straight channel of 150 mm length where a series of vertical perturbation wires of 0.2 mm diameter are placed 10 mm prior and perpendicular to the concave surface leading edge to pre-set the vortex wavelengths. The leading edge is sharp with an angle of 45°. The free-stream turbulence levels in the test section are less than 0.45% for free-stream velocities (U_∞) of 1.0 to 4.0 m/s.

The spanwise spacing between the wires was set to λ_m, which is the most amplified wavelength of Görtler vortices. In this case, U_∞ was determined so that the wavelength parameter $\Lambda = (U_\infty \lambda_m / \nu) (\lambda_m / R)^{0.5} = 250$, where ν is the fluid kinematic viscosity (Mitsudharmadi *et al*., 2004; Tandiono *et al*., 2008). Three values of λ_m were considered: 1) $\lambda_m = 12$ mm, for which $U_\infty = 2.8$ m/s, 2) $\lambda_m = 15$ mm, for which $U_\infty = 2.1$ m/s, and 3) $\lambda_m = 20$ mm, for which $U_\infty = 1.3$ m/s.

A single hot-wire probe operated in Constant Temperature Anemometer system (Dantec 55P15) with a 5 μm diameter (d) and 1.0 mm length (l) tungsten wire was used to obtain mean and fluctuating streamwise velocity data at some streamwise (x) locations. Five pairs of vortices were detected by the hot-wire measurement with 1.0 mm traversing step in the spanwise (z) direction and 0.5-1.0 mm step

in the normal (y) direction inside boundary layers. Mean streamwise velocity (u) contours were then plotted to locate the upwash and downwash regions. The velocity profiles were obtained by measuring u in boundary layer at those locations with 0.5 mm step.

The wall shear stress τ_w was obtained by measuring u very near to the wall to capture the region where the velocity profile is linear. This region is henceforth referred to "linear" layer. The hot-wire probe was initially placed very near to the concave surface with the aid of a camera. The measurement of u was performed with 50 μm step across the boundary layer for 40 points ranging from y = 0.05 to 2.00 mm. Three pairs of vortices were used in this near-wall streamwise velocity measurement with 2.0 mm traversing step along the z-direction.

Calibration checks were regularly performed to ensure that the drift was within ±1%, otherwise the data obtained were rejected, resulting in a re-calibration of the hot-wire.

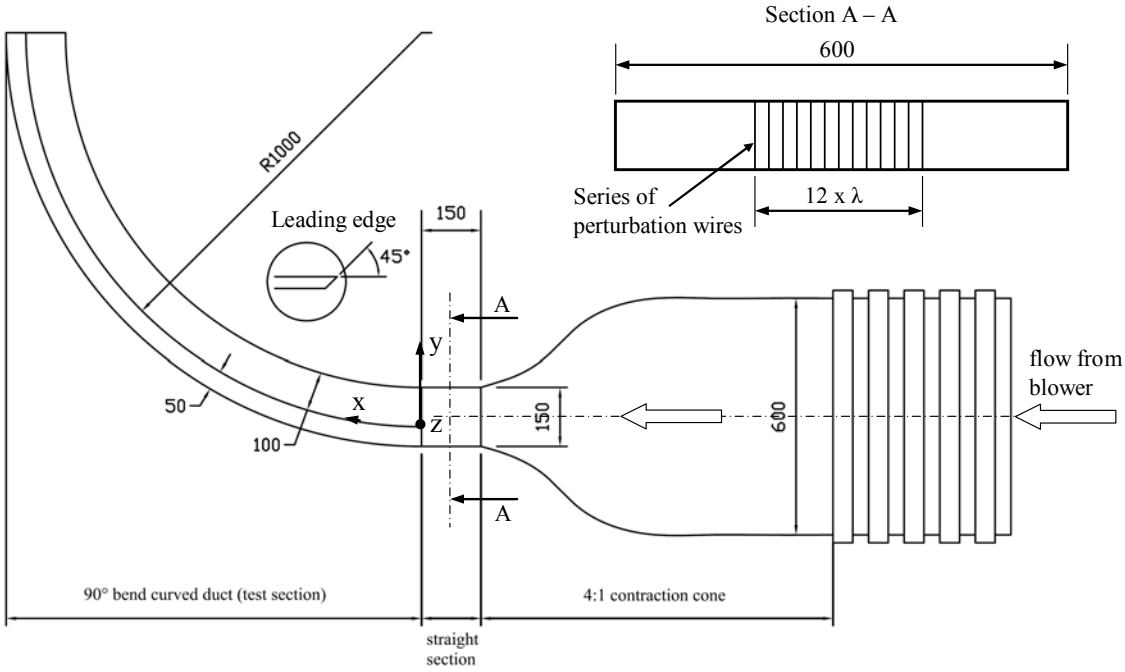

Fig. 1 Schematic of experimental set-up (all dimensions are in mm)

NEAR-WALL VELOCITY GRADIENT TECHNIQUE

To measure wall shear stress in the boundary layer using the mean velocity gradient at the wall is essentially to accurately obtain the velocity profile near the wall. The gradient of the line fitted to the linear portion of the velocity profile is assumed to be the same as the gradient at the wall, and is then used to estimate the wall shear stress $\tau_w = \mu(du/dy)_{y=0}$, where μ is the fluid dynamic viscosity, u the streamwise velocity, and y the normal distance from the wall. It is well established that the viscous sublayer, which extends to a value of $y^+ \approx 5$, exists in all turbulent flows and the velocity gradient in this region is linear (Azad and Burhanuddin, 1983). Hence, the expression of τ_w can be used to estimate the wall shear stress in concave surface laminar and turbulent boundary layer flows.

To accurately measure the velocity near the wall, some difficulties may arise, for example, when the hot-wire probe is traversed into near-wall proximity, the undesired conductive heat transfer from the hot-wire to the wall may give rise to the spurious increase in velocity. The wall effect on the spurious velocity measurements extends to a certain distance from the wall depending on the thermal conductivity of the wall material and the dimension of the hot-wire probe. For a low thermal conductivity material, for example plexiglass, the wall effect extends to $y^+ \approx$ 2.0-3.5 in turbulent boundary layer, and higher for the material with a larger thermal conductivity (Polyakov and Shindin, 1978; Ligrani and Bradshaw, 1987a; Hutchins and Choi, 2002). On the other hand, the velocity profile in a turbulent boundary layer is believed to be linear only up to $y^+ \approx 5$. Hence, the remaining "linear"

layer that is useful to estimate the wall shear stress from the velocity gradient becomes very thin.

Swearingen and Blackwelder (1987) and Ajakh *et al*. (1996) show that the velocity profiles in Görtler vortex flow at both upwash and downwash do not follow either the laminar or turbulent profiles. This makes it difficult to determine the "useful" linear region to estimate the velocity gradient at the wall. Fortunately, the region with the linear velocity gradient in concave surface boundary layer prior to turbulence, as shown in Fig. 2, is sufficiently thick to estimate τ_w by near-wall velocity gradient technique. The least-squares linear fit was then used to estimate the velocity gradient.

Figure 2 shows typical velocity data within 2.0 mm from the wall at upwash and downwash at x = 200 mm of case 2 (λ_m = 15 mm and U_∞ = 2.1 m/s). At this particular x location, the useful linear regions are in the range of 0.65 mm ≤ y ≤ 2.00 mm for upwash and 0.50 mm ≤ y ≤ 1.50 mm for downwash, which correspond to $3 \le y^+ \le 8$ in wall units for both. These limits were determined based on the highest value of the Pearson product-moment correlation coefficient (r) with at least 10 data points involved in the least-square linear fitting. The minimum value of r for these data is 0.99.

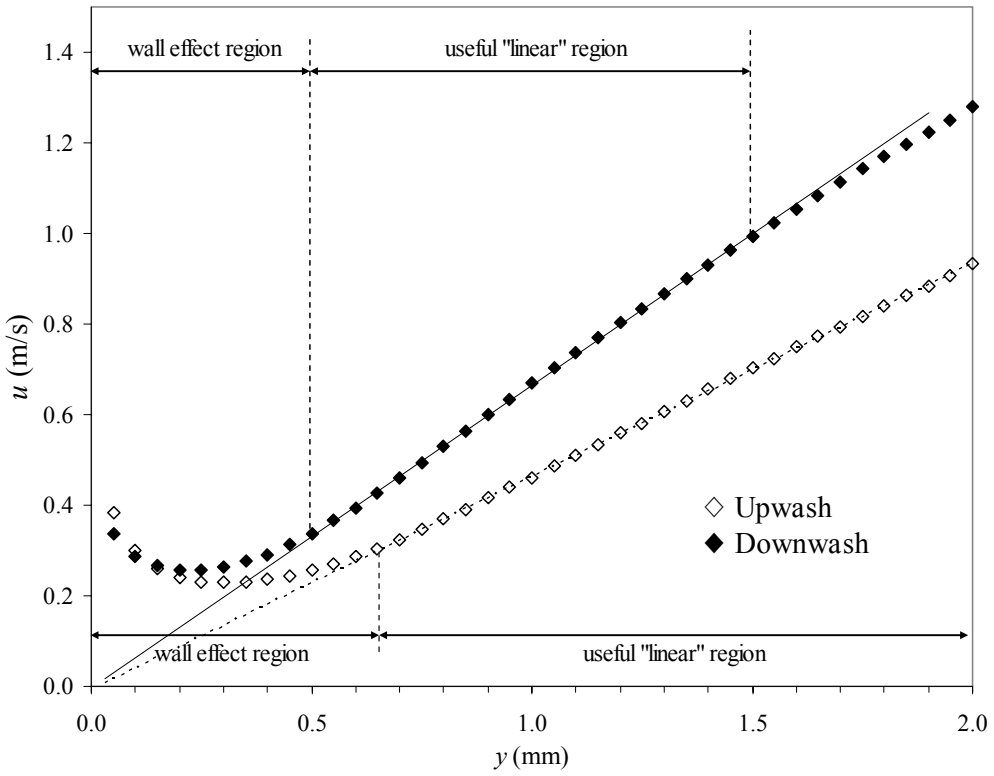

Fig. 2 A typical result of near-wall streamwise velocity measurements at upwash and downwash for case 2: λ_m = 15 mm and U_∞ = 2.1 m/s.

Since the near-wall velocity gradient technique only needs the velocity gradient at the linear region to estimate τ_w, the error due to the probe wall positioning is therefore insignificant, and the main contribution to the error is due to the gradient fit. The least-square linear fit was applied to the near-wall velocity gradient technique to obtain the standard skin friction coefficient error. The standard error in velocity gradient was estimated following Box *et al*. (1978). The present experimental results give a maximum standard gradient error of 3.3 %.

By using a camera with zoom facility, the starting position of the hot-wire probe was ensured to be very near from the concave surface. Then one can rely on the fine-scale traverse mechanism for the subsequent velocity measurement across boundary layer. The positional accuracy of the probe was approximated by the intercept of the line fitted from the linear region of the velocity profile with the x-axis (wall-normal distance). It is found to be within ±28 μm for x = 200 mm of case 2, which is similar to the errors of ±25 μm reported using positioning method by mechanical probe stop (Brunn, 1995).

RESULTS AND DISCUSSION

For a flat plate laminar boundary layer, τ_w decreases with $x^{1/2}$ and increases with $U_\infty^{3/2}$ as the boundary layer grows. However, in Görtler vortex flow, τ_w varies in the spanwise direction like the velocity profile. The streamwise developments of τ_w in term of its coefficient C_f ($\equiv \tau_w / 0.5\rho U_\infty^2$, where ρ is the fluid density) for case 2 (λ_m = 15 mm and U_∞ = 2.1 m/s) are shown in Fig. 3 at upwash and downwash regions together with the spanwise-averaged values. The τ_w curves for the Blasius and flat plate turbulent boundary layer flows are also included for comparison.

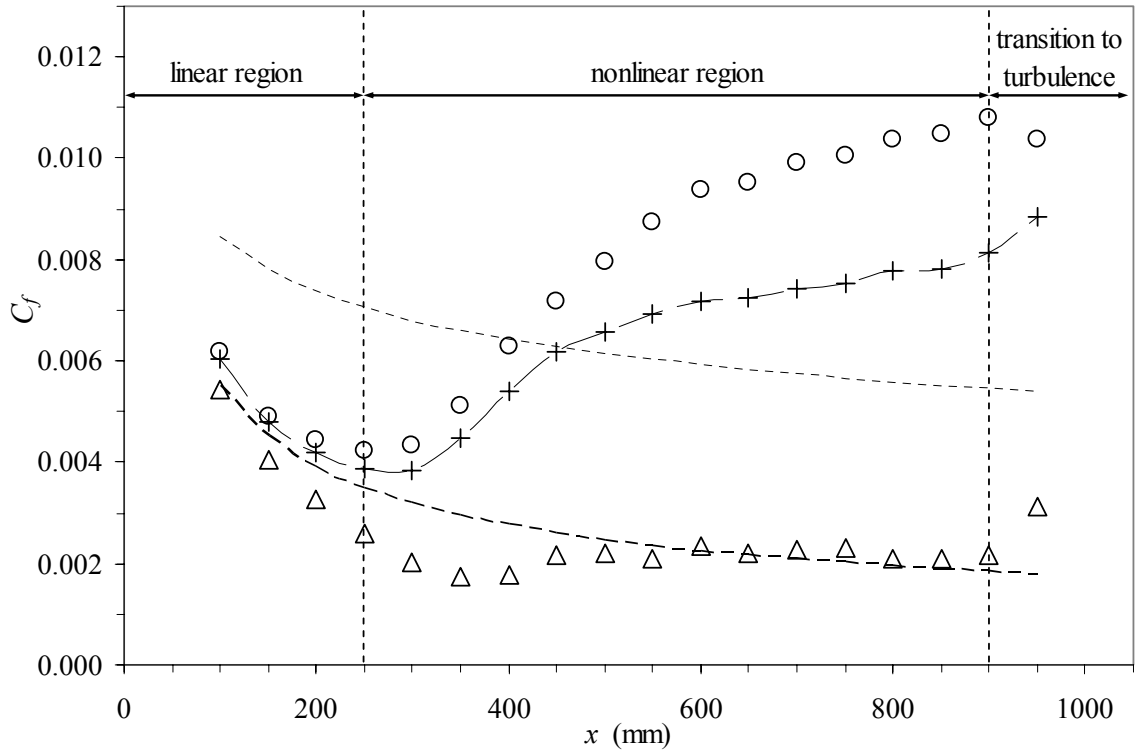

Fig. 3 Wall shear stress coefficient C_f for case 2: λ_m = 15 mm and U_∞ = 2.1 m/s (Δ: at upwash, o : at downwash, − + − : spanwise-averaged value $\overline{C}_f$, —— : Blasius boundary layer, ----- : turbulent boundary layer).

τ_w at upwash decreases faster than the Blasius curve until x = 350 mm (Fig. 3). After reaching its minimum point, that is 59% of Blasius value at that position, it increases downstream to reach the Blasius curve. Further downstream, τ_w follows the Blasius curve closely until the decay of the mushroom-like structures at x = 850 mm. Cases 1 and 3 also show the similar trend that there is a range of streamwise (x) distance in the nonlinear region where the wall shear stress at upwash follows the Blasius curve before the flow becomes turbulent. In contrast to the present results, τ_w obtained by Swearingen and Blackwelder (1987) at upwash simply crossed the Blasius curve after reaching its minimum point, instead of following the curve. This might be due to their coarse hot-wire measurements where only 10 streamwise velocities were measured across boundary layer and the nearest point to the wall was 1.0 mm. Please note that Swearingen and Blackwelder (1987) measured in naturally developing Görtler vortices.

At downwash region, τ_w initially decreases at the rate slightly lower than the Blasius curve, but at x = 250 mm it starts to increase significantly downstream until x = 550 mm. Subsequently, the increasing rate reduces abruptly at x = 900 mm.

The spanwise-averaged curve in Fig. 3 also shows that τ_w starts to increase from x = 300 mm. Computational studies (Sabry and Liu, 1991; Lee and Liu, 1992; Girgis and Liu, 2006) explained that further enhancement of τ_w is due to the effect of nonlinear steady longitudinal Görtler vortices. In the absence of the secondary instability, the spanwise-averaged wall shear stress coefficient $\overline{C}_f$ has

already appeared to a large extent to bridge the Blasius curve and the flat-plate turbulent boundary layer curve. The presence of the secondary instability is to further increase $\overline{C}_f$ well beyond the turbulent values (Girgis and Liu, 2006).

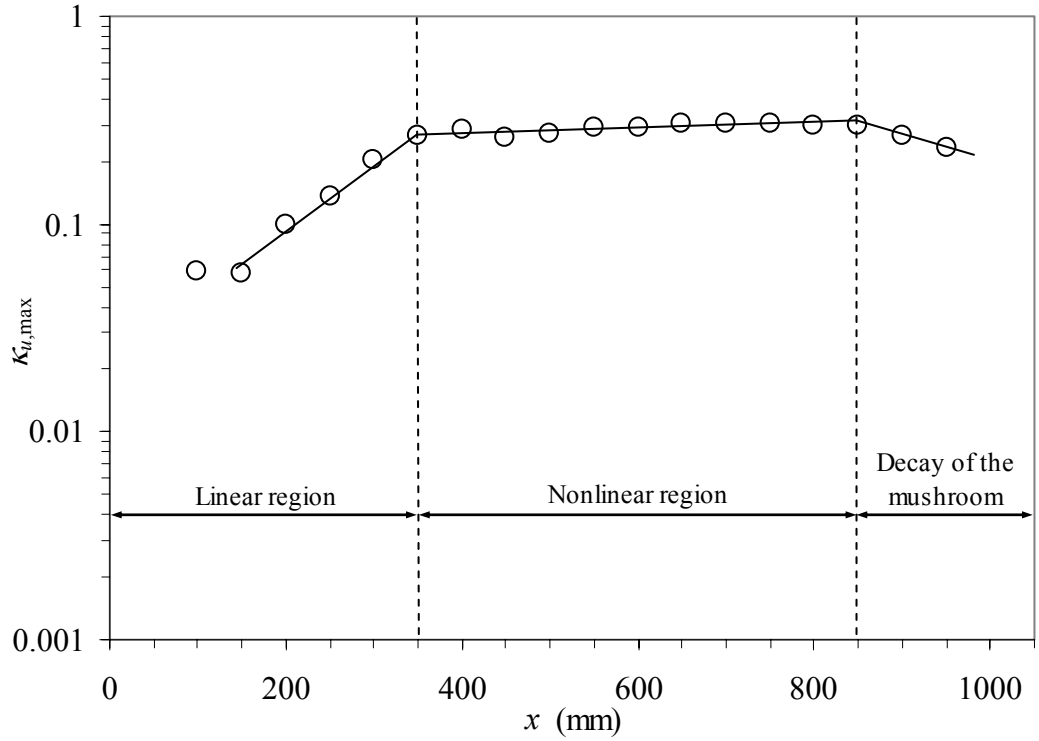

Fig. 4 Development of maximum disturbance amplitude ($\kappa_{u,max}$) for case 2: λ_m = 15 mm and U_∞ = 2.1 m/s showing three different regions (Mitsudharmadi *et al.*, 2004): linear region, nonlinear region, and decay of the mushroom structures.

To quantify the growth of the vortices in term of the mean streamwise velocity component, a vortex or disturbance amplitude κ_u was defined by Winoto and Crane (1980). As discussed earlier, the minimum τ_w at upwash occurs at x = 350 mm (Fig. 3), which is coincidentally the same location where the growth of the maximum disturbance amplitude $\kappa_{u,max}$ ceases and approaches a plateau (Fig. 4). This location is assumed to be the onset of nonlinear region of Görtler vortices (Mitsudharmadi *et al.*, 2004). However, Bottaro and Klingmann (1996) showed that the secondary instability occurs slightly upstream of the location where τ_w at upwash is minimum, which is at slightly upstream of x = 350 mm. These two findings seem to contradict since it is not possible that the secondary instability occurs before the onset of the nonlinear region. The flow becomes susceptible to the secondary instability only after it is sufficiently nonlinear and the energy saturates at a constant level. Therefore, the use of the maximum disturbance amplitude curve, as shown in Fig. 4 for case 2 in this work, to predict the linear and nonlinear regions of Görtler instability may not be accurate. The wall shear stress data may provide a better indication of the onset of the nonlinear region since it is more sensitive than the $\kappa_{u,max}$.

Based on the development of $\overline{C}_f$ in Fig. 3, three different regions can be identified: linear, nonlinear, and transition to turbulence regions. In the linear region, $\overline{C}_f$ still follows the Blasius curve, and the instability, as well as the perturbation energy, grows linearly. The nonlinear region is defined from the streamwise distance where $\overline{C}_f$ begins to depart from the Blasius curve (at x = 250 mm). The perturbation energy grows nonlinearly and finally reaches a saturation level where the flow becomes susceptible to the secondary instability. Lastly, the transition to turbulence region is shown by the increase and decrease of C_f at upwash and downwash respectively, eventually to converge to the same value, indicating the onset of the transition to turbulence and its consequence of increased mixing. The $\overline{C}_f$, as well as the turbulent intensity at upwash and downwash, in this region increase significantly.

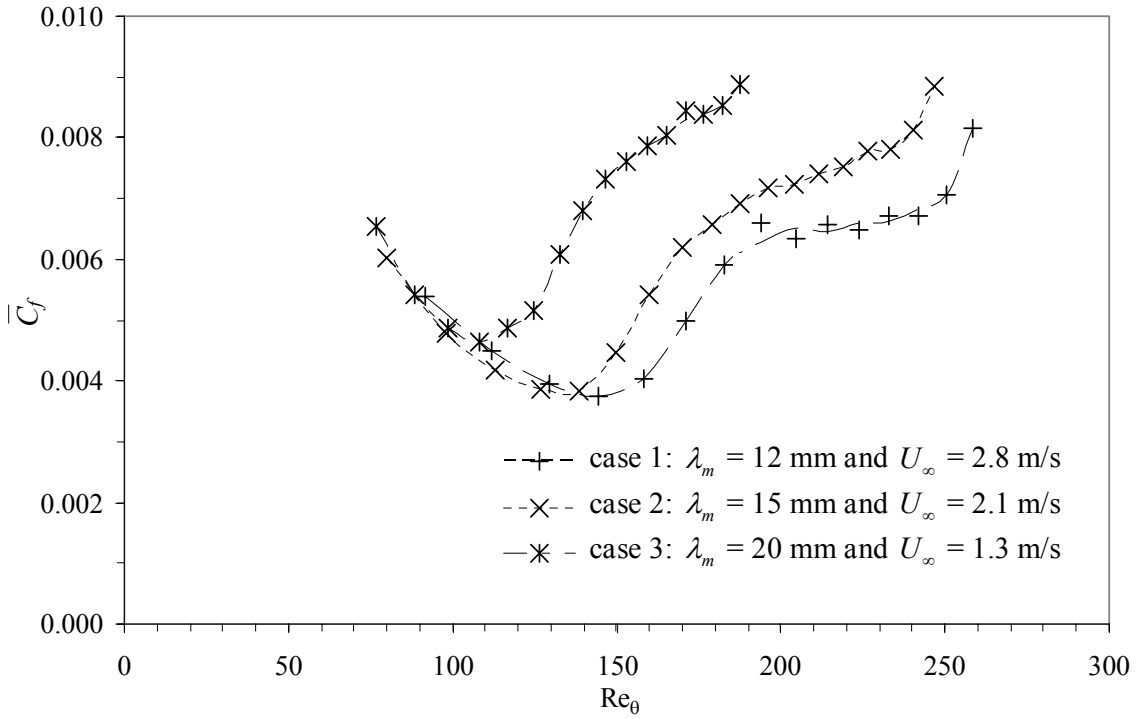

Fig. 5 $\overline{C}_f$ versus Reynolds number Re_θ for case 1: λ_m = 12 mm and U_∞ = 2.8 m/s, case 2: λ_m = 15 mm and U_∞ = 2.1 m/s, and case 3: λ_m = 20 mm and U_∞ = 1.3 m/s.

The streamwise developments of the spanwise-averaged τ_w for all the three cases are shown in Fig. 5, presented as $\overline{C}_f$ and the streamwise (x) distance as Reynolds number Re_θ (= $U_\infty\theta/\nu$), where θ is the Blasius boundary layer momentum thickness. As shown in Fig. 5, $\overline{C}_f$ first decreases and then increases downstream for the three cases. Prior to the minima, $\overline{C}_f$ for all cases seems to follow the same line. The values of Re_θ at the minima are respectively 150, 140, and 110 for case 1, 2, and 3. These locations correspond to the same Gortler number $G_\theta \approx 4.0$. After their minima, the $\overline{C}_f$ values significantly increase downstream until Re_θ of 180, 170, and 140 for case 1, 2, and 3, respectively. These Re_θ values also correspond to the same Gortler number $G_\theta \approx 6.0$. This significant increase is due to the nonlinear effect and the appearance of secondary instability. Downstream of these positions, the rate of increase of $\overline{C}_f$ reduces for a finite range of Re_θ before a steep increase again as a result of increased mixing due to the onset of flow transition to turbulence.

As shown in Fig. 5, the minimum $\overline{C}_f$ of larger vortices occurs at lower Re_θ. After reaching their minima, larger vortices consistently produce higher wall shear stress at any value of Re_θ. These may be due to the fact that larger vortices are more "vigorous" (Bottaro *et al*., 1996). In addition, Gortler vortex wavelength also has a direct influence to the type of the secondary instability mode, which of course will affect the development of the wall shear stress (Li and Malik, 1995).

Associated with the nonlinear region of Görtler vortices, the spanwise distributions of u/U_∞ become distorted such that the downwash becomes flat and the upwash becomes narrow and sharp (Aihara, 1976), as shown in Fig. 6 at $y = 0.5\delta_L$ (where δ_L is Blasius boundary layer thickness) at some x positions. There is a tendency of wavy velocity distribution to approach a finite amplitude, which can be quantified by the maximum disturbance amplitude $\kappa_{u,max}$, as the flow becomes sufficiently nonlinear. The maximum value of $\kappa_{u,max}$ was reported to be from 0.3 to 0.4 (Winoto and Crane, 1980).

As the growth of the vortices in the y direction reaches a finite amplitude, the spanwise distribution of u/U_∞ is then inflected, as shown in Fig. 6(c) and (d), and the flow is dominated by the mushroom-like structures. The inflected velocity profiles in the spanwise direction, as well as the inflected velocity profiles across the boundary layer which occur earlier, indicate the appearance of the

secondary instability. Further investigation reveals that it is related to the sinuous mode of secondary instability (Swearingen and Blackwelder, 1987).

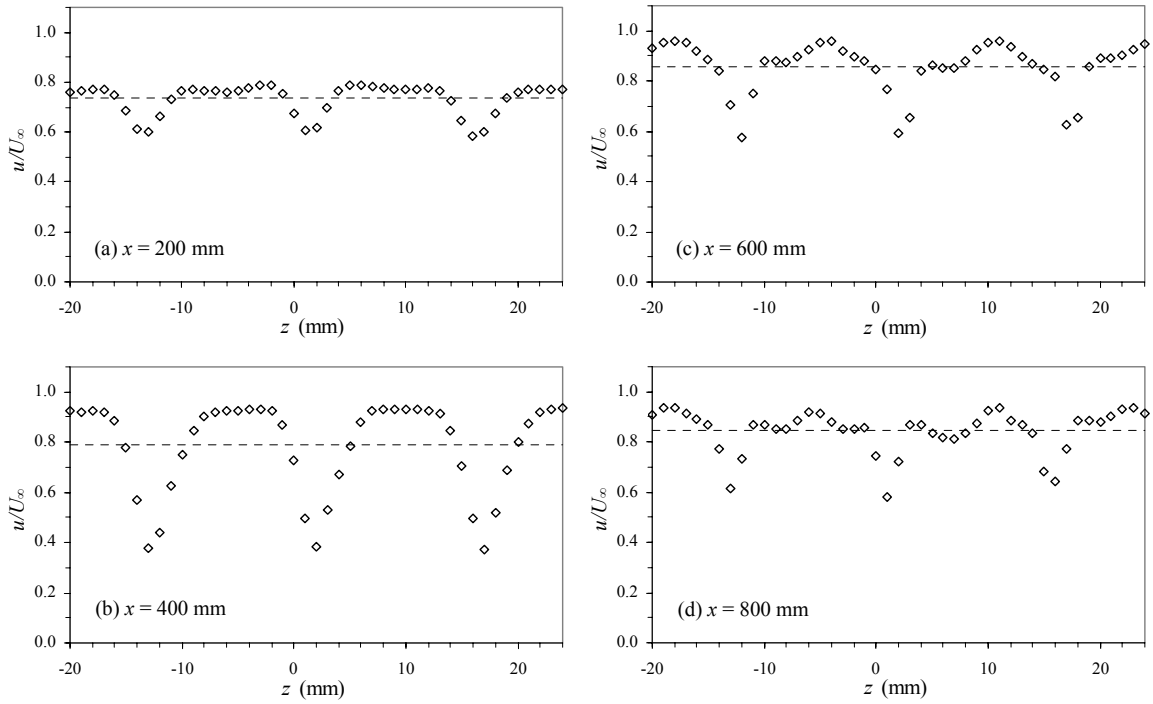

Fig. 6 Spanwise distributions of u/U_∞ for case 2: λ_m = 15 mm and U_∞ = 2.1 m/s at y = 0.5δ_L (---- is spanwise-averaged value of u/U_∞ at corresponding x position).

The spanwise distributions of τ_w in term of C_f at some streamwise positions are shown in Fig. 7. Initially, the spanwise distributions of C_f and u/U_∞, seem to be correlated, as shown in Fig. 6 (a) and 7(a). Further downstream, there is no indication of the spanwise distribution of C_f to become flat at the downwash and narrow or sharp at the upwash, as observed in the spanwise distribution of u/U_∞. Instead, the C_f distribution at the downwash region becomes narrower, and there is no inflection point found in the distribution. This may be because the sinuous mode of secondary instability, which is initiated near the boundary layer edge, is not strong enough to alter the distribution of the τ_w. This also explains why the increasing rate of C_f (in Fig. 3) reduces significantly prior to the flow transition to turbulence. The main contribution to the enhancement of τ_w in a concave surface boundary layer flow may be attributed to the varicose mode of the secondary instability. This is concluded from the fact that the waviness in C_f distribution becomes more pronounced and the spanwise-averaged value $\overline{C}_f$ increases significantly at the early stage of the nonlinear region where the flow instability, in the present work, is still dominated by the varicose mode.

CONCLUSIONS

The streamwise development of τ_w in Görtler vortex flows has been investigated on a concave surface of R = 1.0 m for three different vortex wavelengths and free-stream velocities, but the same wavelength parameter Λ of 250. Streamwise velocity measurements were carried out using hot-wire anemometry and τ_w data were obtained by using the near-wall velocity gradient technique with a very fine step-size.

τ_w at downwash decreases at a slightly lower rate than the Blasius curve, and subsequently increases after reaching its minimum point. In contrast, τ_w at upwash decreases at a higher rate than the Blasius curve. The minimum τ_w is found to be 59% of the Blasius value at that position. After reaching its minimum point, τ_w increases slightly due to the secondary instability as the onset of secondary instability is just slightly before the location of the minimum τ_w at the upwash (Bottaro and Klingmann,

1996). The $\overline{C}_f$, which initially follows the Blasius curve, increases well above the local turbulent boundary layer value further downstream due to the nonlinear effects of Görtler instability and the secondary instability modes.

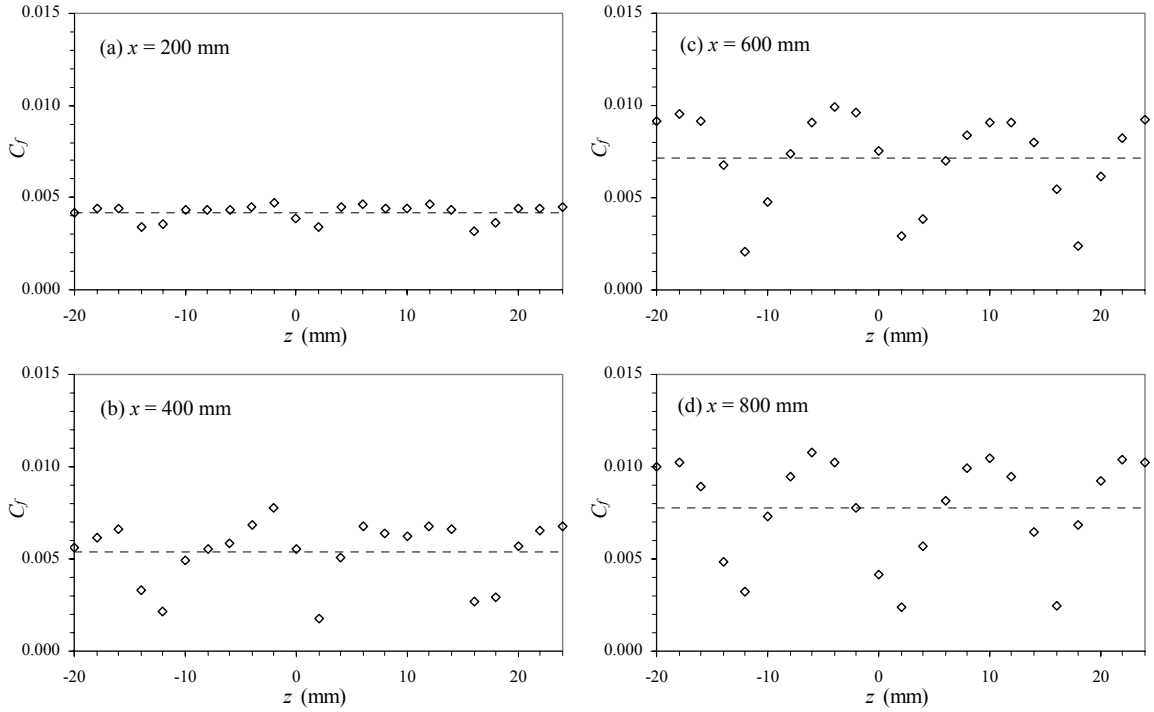

Fig. 7 Spanwise distributions C_f for case 2: λ_m = 15 mm and U_∞ = 2.1 m/s (----- is spanwise-averaged value $\overline{C}_f$ at corresponding streamwise position).

The τ_w data provides a more accurate indication of the onset of nonlinear region than the $\kappa_{u,max}$ criterion (Mitsudharmadi *et al*., 2004) and three different regions can be identified based on the streamwise development of $\overline{C}_f$. The onset of the nonlinear region is defined as the streamwise location where $\overline{C}_f$ starts to depart from the Blasius curve. The transition to turbulence is initiated by a significant increase in $\overline{C}_f$. At the same time, τ_w at upwash also drastically increases, but it decreases at downwash as a result of increased mixing due to turbulence.

Unlike the spanwise distribution of streamwise velocity, that of C_f becomes narrower at downwash in the nonlinear region, and no inflection point found further downstream. This may be because the sinuous mode of the secondary instability is not strong enough to alter the spanwise distribution of the τ_w. The reduction in the rate of increase of $\overline{C}_f$ in the later part of the nonlinear region, where the instability is dominated by the sinuous mode, suggests that the main contribution to the enhancement of τ_w in Görtler vortex flow may come from the varicose mode of the secondary instability.

REFERENCES

Aihara, Y. (1976), "Nonlinear analysis of Görtler vortices", Physics of Fluids **19** (11), 1655.

Ajakh, A., M. Kestoras, and H. Peerhossaini (1996), "Experiments on the Görtler instability: its relation to transition to turbulence", in *Proceedings of the 1996 ASME Fluids Engineering Division Summer Meeting. Part 2 (of 3)*, *San Diego*, *1996* (ASME, New York, 1996), 613-621.

Alfredsson, P. H., A. V. Johansson, J. H. Haritonidis, and H. Eckelmann (1988), "The fluctuating wall shear stress and the velocity field in the viscous sublayer", Physics of Fluids **31** (5), 1026.

Azad, R.S. and S. Burhanuddin (1983), "Measurements of some features of turbulence in wall-proximity", Experiments in Fluids **1** (3), 149.

Bhatia, J. C., F. Durst, and J. Jovanovic (1982), "Corrections of hot-wire anemometer measurements near walls", Journal of Fluid Mechanics **122**, 411.

Bottaro, A. and B. G. B. Klingmann (1996), "On the linear breakdown of Görtler vortices", European Journal of Mechanics, B/Fluids **15** (3), 301.

Bottaro, A., B. G. B. Klingmann, and A. Zebib (1996), "Goertler vortices with system rotation", Theoretical and Computational Fluid Dynamics **8** (5), 325.

Box, G. E. P., W. G. Hunter, and J. S. Hunter (1978), Statistics for experimenters: an introduction to design, data analysis, and model building, John Wiley & Sons, Inc., New York, USA.

Bruun, H.H. (1995), Hot-wire anemometry: principles and signal analysis, Oxford Unversity Press, Oxford, UK.

Chew, Y. T., B. C. Khoo, and G. L. Li (1994), "A time-resolved hot-wire shear stress probe for turbulent flow: use of laminar flow calibration", Experiments in Fluids **17** (1-2), 75.

Girgis, I. G. and J. T. C. Liu (2006), "Nonlinear mechanics of wavy instability of steady longitudinal vortices and its effect on skin friction rise in boundary layer flow", Physics of Fluids **18** (2), 024102.

Görtler, H. (1940) "Über eine dreidimensionale Instabilität laminarer Grenzschichten an konkaven Wänden, Gesellschaft der Wissenschaften zu Göttingen, Nachrichten", Mathematik, **2**, 1.

Hall, P. and N. J. Horseman (1991), "Linear inviscid secondary instability of longitudinal vortex structures in boundary layers", Journal of Fluid Mechanics **232**, 357.

Hanratty, T. J. and J. A. Campbell (1983), "Measurement of wall shear stress", in *Fluid mechanics measurements*, edited by R. J. Goldstein, Hemisphere Publishing, Washington DC, 559-615.

Hutchins, N. and K.-S. Choi (2002), "Accurate measurements of local skin friction coefficient using hot-wire anemometry", Progress in Aerospace Sciences **38** (4-5), 421.

Lee, K. and J. T. C. Liu, "On the growth of mushroomlike structures in nonlinear spatially developing Goertler vortex flow", Physics of Fluids A: Fluid Dynamics **4** (1), 95 (1992).

Li, F. and M. R. Malik (1995), "Fundamental and subharmonic secondary instabilities of Görtler vortices", Journal of Fluid Mechanics **297**, 77.

Ligrani, P. M., and P. Bradshaw (1987a), "Subminiature hot-wire sensors: development and use", Journal of Physics E: Scientific Instruments **20** (3), 323.

Ligrani, P. M. and P. Bradshaw (1987b), "Spatial resolution and measurement of turbulence in the viscous sublayer using subminiature hot-wire probes", Experiments in Fluids **5** (6), 407.

Mitsudharmadi, H., S. H. Winoto, and D. A. Shah (2004), "Development of boundary-layer flow in the presence of forced wavelength Görtler vortices", Physics of Fluids **16** (11), 3983.

Polyakov, A.F. and S. A. Shindin (1978), "Peculiarities of hot-wire measurements of mean velocity and temperature in the wall vicinity", Heat and Mass Transfer **5** (1), 53.

Sabry, A. S. and J. T. C. Liu (1991), "Longitudinal vorticity elements in boundary layers. Nonlinear development from initial Goertler vortices as a prototype problem", Journal of Fluid Mechanics **231**, 615.

Swearingen, J. D. and R. F. Blackwelder (1987), "Growth and breakdown of streamwise vortices in the presence of a wall", Journal of Fluid Mechanics **182**, 255.

Tandiono, S. H. Winoto, and D. A. Shah (2008), "On the linear and nonlinear development of Görtler vortices ", Physics of Fluids **20** (9), 094103.

Winoto, S .H. and R. I. Crane (1980), "Vortex structure in laminar boundary layers on a concave wall", International Journal of Heat and Fluid Flow **2** (4), 221.

Winter, K.G. (1979) "An outline of the techniques available for the measurement of skin friction in turbulent boundary layers", Progress in Aerospace Sciences **18**, 1.